HHS Public Access

Author manuscript

Nat Med. Author manuscript; available in PMC 2017 March 05.

Published in final edited form as:

Nat Med. 2016 October ; 22(10): 1170–1179. doi:10.1038/nm.4166.

Serotonin reuptake inhibitors act centrally to cause bone loss in mice by counteracting a local antiresorptive effect

María José Ortuño[1], **Samuel T. Robinson**[2], **Prakash Subramanyam**[3], **Riccardo Paone**[1,4], **Yung-yu Huang**[5], **X. Edward Guo**[2], **Henry M. Colecraft**[3], **J. John Mann**[5], and **Patricia Ducy**[6]

[1]Department of Genetics & Development, College of Physicians & Surgeons, Columbia University, New York, NY, USA

[2]Department of Biomedical Engineering, Columbia University, New York, NY, USA

[3]Department of Physiology and Cellular Biophysics, Columbia University, New York, NY, USA

[4]Department of Biotechnological and Applied Clinical Sciences, University of L'Aquila, L'Aquila, Italy

[5]Department of Psychiatry, College of Physicians & Surgeons, Columbia University, New York, NY, USA

[6]Department of Pathology & Cell Biology, College of Physicians & Surgeons, Columbia University, New York, NY, USA

Abstract

The use of selective serotonin reuptake inhibitors (SSRIs) has been associated with an increased risk of bone fracture, raising concerns about their increasingly broader usage. This deleterious effect is poorly understood and thus strategies to avoid this side effect remain elusive. We show here that fluoxetine (Flx), one of the most prescribed SSRI, acts on bone remodeling through two distinct mechanisms. Peripherally, Flx has antiresorptive properties, directly impairing osteoclast differentiation and function through a serotonin reuptake-independent Ca^{2+}-calmodulin-NFATc1-dependent mechanism. With time, however, Flx also triggers a brain serotonin-dependent rise in sympathetic output that increases bone resorption sufficiently to counteract its local antiresorptive effect; thus leading to a net effect of impaired bone formation and bone loss. Accordingly, neutralizing this second mode of action through co-treatment with the β-blocker propranolol, while leaving the peripheral effect intact, prevents Flx-induced bone loss in mice. Hence, this study identifies a dual mode of action of SSRIs on bone remodeling and suggests a therapeutic strategy to block the deleterious effect on bone homeostasis from their chronic use.

Correspondence should be addressed to: Patricia Ducy, pd2193@cumc.columbia.edu.

Author contribution

P.D. conceived the study; M.J.O. performed most of the experiments; S.T.R. performed the micro-CT analysis under X.E.G. supervision; P.S. assisted with the calcium signaling analysis under H.C. supervision; R.P. assisted with the histomorphometry analysis; Y.-Y.H performed the HPLC analysis under J.J.M. supervision. M.J.O., H.M.C., J.J.M and P.D. analyzed and discussed the results. M.J.O. and P.D. wrote and revised the manuscript.

Competing financial Interest

Authors declare no competing financial interest.

Selective serotonin reuptake inhibitors (SSRIs) and among them fluoxetine (Flx), the active compound in Prozac, are the most widely prescribed antidepressants in western countries. Their therapeutic effect is mediated by a central increase of serotonin signaling in post-synaptic neurons due to an inhibition of serotonin reuptake by the 5-hydroxytryptamine transporter (5HTT) expressed by pre-synaptic neurons[1,2]. Given their remarkable binding specificity for 5HTT, SSRIs have progressively been favored over less-targeted antidepressants because they decrease the potential for unwanted side effects. They are also increasingly prescribed to treat non-psychiatric disorders, including preventing hot flashes in menopausal women[3,4].

In recent years, however, multiple clinical studies have reported a positive association between the use of SSRIs and a decrease in bone mineral density and (or) an increased risk of fractures, raising considerable concern about their broad use[5–7]. This association between SSRI treatment and bone loss was confirmed in multiple rodent models[8–11]. As these animal studies bypass a major confounding issue of the clinical analyses, namely the fact that SSRIs are prescribed to depressed individuals and that depression is by itself a possible cause for bone loss[5,6,12], they have strengthened the notion that treatment with SSRIs could be an independent risk factor for developing osteoporosis. Yet, despite noting a decrease in bone formation[8–10] these animal studies did not identify the molecular mechanism for this effect on bone or a therapeutic strategy to prevent or treat this side effect. These animal studies also did not explain why chronic administration of SSRIs causes bone loss while these drugs are designed to increase central serotonin signaling, a pathway known to favor bone mass accrual[13,14]. To explain this paradox and define the action of SSRIs on bone remodeling at the molecular level we analyzed the effect of chronic treatments of various length on normal, healthy mice. Here, we identify a dual mode of action of Flx on bone remodeling that provides a molecular explanation for its observed effects on bone. In particular, we show that a short-term (3 weeks) treatment with Flx results in a local anti-resorptive response that increases bone mass, but that there is a net loss of bone with longer-term (6 weeks) Flx use, which is mediated by a centrally-triggered increase in sympathetic activity. Based on these findings we then show that co-treating mice with Flx and a β-blocker can prevent this deleterious side effect.

Results

The extent of SSRIs use determines their impact on bone mass

Clinical studies reporting bone loss following treatment with SSRIs examined individuals that took these drugs for a relatively long period of time (≥ one year). However, in the rare cases that these analyses were performed after only a few months of treatment an improved bone density and a decrease in bone resorption parameters have been reported[15–17]. To test if the length of treatment correlates with different effects of SSRIs on bone remodeling we treated wild-type (WT) female mice for 3 (3 w) or 6 weeks (6 w) with a dose of Flx resulting in plasma concentrations similar to the therapeutic levels achieved in humans[18]. In both long bones and vertebrae, the longer-term treatment caused bone loss while mice treated with Flx for the shorter time showed a higher bone volume (BV/TV, bone volume over tissue volume) than vehicle (veh)-treated mice (Fig. 1a).

To understand the cellular basis underlying this time-dependent effect we performed bone histomorphometry. Mice treated for only 3 w with Flx showed lower osteoclast surface (Oc.S/BS, osteoclast surface over bone surface) while bone formation rate (BFR/BS, bone formation rate over bone surface) and osteoblast surface (Ob.S/BS, osteoblast surface over bone surface) were not significantly affected compared to veh-treated mice (Fig. 1b,c). Accordingly, the concentration of Deoxypyridinoline crosslinks (Dpd), a marker of bone resorption, was lower in Flx-treated than in veh-treated mice while concentration of osteocalcin (OCN), a marker of bone formation, was not (Fig. 1d). In mice treated for 6 w with Flx, however, histomorphometry and biomarker analysis showed that the osteoclast parameters that were significantly lower after 3 w of treatment compared to the veh-treated group were no longer significantly different after 6 w of treatment compared to veh (Fig. 1b,d,e,f). In contrast, osteoblast parameters such as bone formation rate and OCN concentration that were not significantly different after 3 w of Flx treatment versus veh were lower following 6 w of treatment with Flx compared to veh (Fig. 1c,d,f,g).

Flx directly impairs osteoclast differentiation and function

To understand the dual effects of Flx on bone resorption with respect to shorter-term versus longer-term use, we first assessed the ratio of expression of *Tnfrsf11b* (also known as Osteoprotegerin, OPG) to *Tnfsf11* (also known as Receptor activator of nuclear factor κ-B ligand, RANKL) in long bones, an indicator of a potent osteoblast-driven pathway regulating osteoclast differentiation and function[19,20]. While this ratio was not significantly affected following 3 w of treatment, it was lower in mice subjected to the longer treatment with Flx compared to veh (Fig. 2a).

To determine if a direct effect on osteoclasts could be a mechanism by which Flx affects bone homeostasis we treated primary osteoclast cultures with a dose of Flx similar to levels observed in plasma and tissues of individuals taking this drug[18]. When mouse primary osteoclast precursors were differentiated in the presence of Flx or other SSRIs such as paroxetine (Paro) and fluvoxamine (Fluvo), the number of differentiated osteoclasts was significantly lower compared to veh-treated cultures (Fig. 2b). Yet, veh- and these SSRIs-treated cultures had a similar number of mononuclear cells suggesting that the viability of the osteoclast precursors was not affected (Fig. 2b). Citalopram (Cita), however, did not show a significant inhibitory effect on osteoclast differentiation suggesting the existence of intra-class differences among different SSRIs (Fig. 2b). The inhibitory effect of Flx on osteoclast differentiation was reversible upon its withdrawal from the culture, further ruling out cell death as the basis for this activity (Fig. 2c). SSRIs treatment also directly affected osteoclast function, as primary cultures already differentiated and treated for 24 hours with Flx, Paro or Fluvo, but not Cita, showed lower tartrate-resistant acid phosphatase (TRAP) activity compared to veh-treated cells (Fig. 2d).

To better understand how Flx influences osteoclast biology we examined the key processes that mark the differentiation of pre-osteoclasts into mature, functional osteoclasts: fusion of mononuclear cells into multinucleated osteoclasts, formation of a specific adhesion structure termed the ruffled border and the ability to resorb mineralized bone[19,20]. Whether added to the culture of osteoclast precursors during the entire differentiation process or only during its

final stage, Flx inhibited cell fusion as indicated by a lower average number of nuclei in TRAP positive multinucleated cells and lower expression of *Dc-stamp* and *Atp6v0d2*, two genes encoding proteins required for this process[19], compared to veh (Fig. 2e,f). Adhesion was also affected since expression of the gene encoding Integrin β3 (*Itgb3*), a key adhesion molecule[19], was specifically lower and the supernatant contained more, TRAP-positive, cells in Flx- than in veh-treated cultures (Fig. 2f,g). These cells were alive since they could be re-plated and cultured (Fig. 2g). In contrast, Flx did not affect the formation of the actin ring or the expression of the genes encoding proteins required for establishing the ruffled border[21,22] (Supplementary Fig. 1). Lastly, we analyzed the effect of Flx on the resorptive capacity of mature osteoclasts. Expression of multiple genes that encode proteins involved in this process such as Cathepsin K or units of the proton pump was lower in Flx- compared to veh-treated cultures, as was pit resorption (Fig. 2h,i). Altogether these data indicate that Flx directly impairs osteoclast fusion, adhesion and resorptive function. Notably, the expression of all genes controlling these processes and found affected by Flx in vitro was lower in mice treated for 3 weeks with this drug than in veh-treated mice (Fig. 2j).

Flx alters calcium signaling in osteoclasts

Given the affinity of SSRIs for the 5HTT transporter and its previously reported expression in osteoclasts[23–25], we next tested whether 5HTT mediates the direct effect of Flx on osteoclast biology. The ability of Flx to inhibit osteoclast differentiation was not impaired in cells derived from mice lacking *Slc6a4*, the gene encoding 5HTT, or from mice lacking *Tph1*, the gene encoding the rate limiting enzyme for serotonin synthesis (*Tph1*$^{-/-}$ mice) as assessed by TRAP activity or gene expression (Fig. 3a and Supplementary Fig. 2a,b). Moreover, following a 3 w treatment with Flx, *Slc6a4*-deficient mice showed a modification of their bone histomorphometry profile similar to WT mice treated for the same amount of time with Flx; i.e., a bone volume higher than veh-treated mice associated with a lower osteoclast surface (Fig. 3b). These observations indicate that Flx directly inhibits osteoclast differentiation and function in a 5HTT-independent manner.

To understand how Flx could directly act on osteoclast biology if not through its canonical mode of action we assessed the expression of key factors controlling osteoclast biology[26]. Expression of *c-Fos* and of its downstream target *Nfatc1* was lower in the presence of Flx than of veh whereas expression of *Cebpa*, which acts upstream of c-Fos in the osteoclast differentiation cascade[27], was not affected (Fig. 3c). Of note, expression of *c-Fos* and *Nfatc1* was lower in Flx- than in veh-treated *Slc6a4*-deficient cells, again showing that Flx acts direct on osteoclast biology independently from 5HTT (Fig. 3d). Expression of *Nfatc1* was also significantly lower in the long bones of WT mice treated for 3 weeks with Flx than with veh (Fig. 3e).

A decrease in *c-Fos* expression could be caused by an inhibition of RANKL signaling through the p38-MAPKinase pathway or by an interference with the Ca^{2+}-calmodulin dependent activation of CREB[28,29]. Western blot analyses did not detect a change in the phosphorylation of p38-MAPK upon Flx compared to veh treatment (Fig. 3f), indicating that direct RANKL signaling is not the main pathway affected. There was, however, significantly lower levels of phosphorylated CREB (p-CREB) in Flx-treated than in veh-treated

osteoclasts (Fig. 3f). Fura-2 calcium imaging experiments confirmed that Flx decreases intracellular Ca^{2+} levels in multinucleated osteoclasts while it does have this effect in mononuclear precursors (Fig. 3g). Moreover W5, a selective antagonist of Ca^{2+}-calmodulin signaling[30], abolished the effect of Flx on the expression of osteoclast differentiation markers as well as on resorptive activity (Fig. 3h,i). Likewise, reducing *Creb* expression through gene inactivation or blocking CREB transcriptional activity with the KG-501 inhibitor[31] mimicked and blocked the negative effect of Flx on these parameters (Fig. 3i and Supplementary Fig. 2c).

Hence, Flx causes its 5HTT-independent inhibitory effect on osteoclast biology by directly impairing a Ca^{2+}/calmodulin-CREB-NFATc1 signaling cascade required for their differentiation and function. This effect is reminiscent of the Ca^{2+} signaling inhibition observed in Jurkat T lymphocytes treated with Flx[32]. We therefore tested whether mice treated with Flx for 3 weeks showed differences in lymphocyte differentiation markers. Indeed, expression of genes encoding Creb and NFAT but also of the master regulator of lymphocyte Th17 differentiation RORγt, a key component of the osteoimmune crosstalk involved in rheumatoid arthritis[33,34], was reduced in the spleen of Flx- compared to veh-treated mice (Fig. 3j). These changes in gene expression occurred independently of the serotonin reuptake process since they could be observed in *Slc6a4*-deficient mice (Fig. 3j).

Flx inhibits brain serotonin signaling to cause bone loss

While a direct, negative, effect of Flx on bone resorption can explain the higher bone mass observed after a 3 w treatment it cannot explain why a longer-term treatment causes bone loss and a decrease in bone formation. Analysis of primary cultures of osteoblasts treated with Flx ruled out a direct effect on these cells since Flx did not induce changes in expression of the genes controlling their differentiation or characterizing their function[35,36] (Supplementary Fig. 3).

In search for an indirect mechanism that could cause bone loss we reckoned that the lower bone resorption compared to veh caused by the direct effect of Flx on osteoclasts was no longer apparent after 6 weeks of treatment. This suggested that another, enhancing, effect on bone resorption was developing when the treatment was extended. Supporting this hypothesis, expression of the gene encoding RANKL and therefore the *Tnfrsf11b*/*Tnfsf11* ratio was changed after 6 but not 3 w of treatment with Flx and *Nfatc1* expression was normalized compared to vehicle after 6 w of treatment (Fig. 2a and Fig. 4a). An increase in RANKL levels could rescue the inhibitory effect of Flx on the Ca^{2+}-calmodulin-NFATc1 pathway by independently activating the RANK-NFκB-NFATc1 cascade[37,38]. To verify that Flx does not affect this parallel activity of RANKL, RAW264.7 osteoclasts were treated with a low and higher dose of RANKL in the presence of Flx or vehicle. In either case, RANKL induced a similar dose-dependent effect: levels of the inhibitor IκBα were lower and NFκB p65 nuclear levels were higher than in control cells (Fig. 4b and Supplementary Fig. 4).

An increase in RANKL-mediated, OPG expression-independent, bone resorption associated with a decrease in bone formation is a hallmark of the effect of sympathetic signaling in osteoblasts[39,40]. We therefore tested whether a longer-term treatment with Flx increased sympathetic output. Indeed, the concentrations of epinephrine (E) and norepinephrine (NE),

the two main effectors of the sympathetic nervous system (SNS), in urine were significantly higher after 6 w but not after 3 w of treatment with Flx compared to veh (Fig. 4c). Likewise, expression of *Ucp1* in brown fat, a marker of SNS activity, was only higher in mice treated with Flx for 6 w compared to 3 w of treatment or veh treatment (Fig. 4d).

We then explored how Flx could affect sympathetic output. Both the hypothalamic expression of *Butyrylcholinesterase* (*Bche*), a gene up-regulated in absence of brain serotonin signaling[14], and the concentration of NE in brainstem extracts were higher in Flx- compared to veh-treated mice (Fig. 4e). These observations suggested that Flx could impair signaling of the central serotonin/Htr2c pathway known to specifically influence bone remodeling[13,14]. Indeed, hypothalamic extracts from mice treated for 6 w with Flx showed significantly lower levels of phosphorylated CREB (p-CREB), a downstream mediator of serotonin signaling through Htr2c[14], compared to mice treated with veh (Fig. 4f). This effect was even more pronounced compared to mice treated for only 3 w with Flx, as these showed the increase in p-CREB hypothalamic levels that Flx is expected to induce upon increasing serotonin signaling (Fig. 4f). A similar biphasic effect could also be observed when Neuro2A neuroblastoma cells that robustly express *Htr2c* were treated with increasing amount of serotonin (Fig. 4g and Supplementary Fig. 5). These data suggest that, by progressively increasing serotonin signaling in the brain, Flx can induce Htr2c desensitization, a classic feature of GPCR signaling[41]. Of note, western blot analyses also showed that levels of Htr2c in hypothalamic extracts became gradually lower after 3 and 6 w of Flx treatment compared to veh (Fig. 4f). These data support the notion that, with time, Flx decreases serotonin signaling in the hypothalamus.

To confirm genetically that the central effect of Flx is serotonin-dependent we treated mice lacking *Tph2*, the gene encoding the enzyme required for brain serotonin synthesis, with Flx or vehicle for 6 weeks. In contrast to the effect observed in WT mice, Flx failed to modify sympathetic output or the *Tnfrsf11b*/*Tnfsf11* ratio in *Tph2*$^{-/-}$ mice (Fig. 4h). As a result, these mutant mice treated with Flx did not show lower bone formation parameters and did not loose bone compare to the veh-treated group (Fig. 4i). Instead, their bone volume was improved compared to veh-treated *Tph2*$^{-/-}$ mice due to a lower osteoclast surface (Fig. 4i). This phenotype, which mimics the one observed in WT mice treated with Flx for 3 w, indicates that in absence of a central effect Flx anti-resorptive peripheral activity persists after 6 w of treatment. A similar improvement in bone volume was observed in *Slc6a4*$^{-/-}$ mice treated for 6 w with Flx compared to veh (Fig. 4j). Thus, Flx does not use another, unexpected and serotonin-independent mechanism than its known action on brain 5HTT to induce bone loss.

Given that most of the clinical data on the effect of SSRIs on bone health were acquired in women, the previous experiments were all performed in female mice. To test if Flx exerts the same action in both genders we next treated groups of male mice with Flx. As in female mice, bone loss could be observed in both vertebrae and long bones after 6 w of Flx compared to veh treatment (Fig. 5a). This effect was due to a lower bone formation, as indicated by a sharp drop of serum OCN concentration (Fig. 5b), while the concentration of the resorption marker Dpd was not statistically different compared to the veh-treated group despite a markedly lowered *Tnfrsf11b*/*Tnfsf11* ratio (Fig. 5c,d). As in female mice, this

phenotype was associated with a trend for higher SNS output, although this did not reach statistical significance for changes in E and NE concentrations (Fig. 5e,f). Likewise, Flx triggered similar inhibitory responses with respect to gene expression and function compared to veh in primary osteoclasts derived from male as from female mice (Fig. 5g–i).

Co-treatment with propranolol prevents Flx-induced bone loss

If the bone loss induced by longer-term Flx use results from an increase in SNS output, then decreasing SNS signaling in bone cells should prevent this side effect. To test this hypothesis we analyzed WT mice co-treated for 6 w with Flx and a low, 0.5 mg/day, dose of propranolol (Prop) that does not significantly affect bone mass accrual by itself (Fig. 6a–d). Compared to mice treated with Flx alone, mice treated with both drugs did not lose bone, showing normal bone formation parameters and lower bone resorption parameters, as assessed by histomorphometry of vertebrae and serum concentration of biomarkers (Fig. 6a–c). Similar results were obtained on tibiae analyzed by microcomputed tomography (μCT) (Fig. 6d). In agreement with the role of sympathetic signaling in osteoblasts[39,40], the *Tnfrsf11b*/*Tnfsf11* ratio, and more specifically the expression of the gene encoding RANKL, was normalized in mice co-treated with Flx and propranolol compared to those treated with Flx alone although their sympathetic tone was similarly high compared to veh- or Prop-treated mice (Fig. 6e–g). Notably, in a marble-burying test we used throughout the study as a functional readout of the effect of Flx on behavior (Supplementary Fig. 6) the co-treatment with a low dose of propranolol did not alter this aspect of Flx activity (Fig. 6h), suggesting that Flx's central action on this behavior was not affected.

Discussion

This study shows that Flx affects bone mass accrual in mice through two distinct mechanisms (Fig. 6i). In particular, Flx can interfere directly with Ca^{2+}/calmodulin signaling in osteoclasts to decrease CREB phosphorylation, *c-Fos* and *Nfatc1* expression thereby impairing the maturation and activity of these cells. This mechanism of action is consistent with the lower bone resorption observed in mice treated with Flx for 3 w compared to the veh-treated group, and is independent of the 5HTT transporter. Upon a longer treatment (6 w), however, this direct inhibitory effect on osteoclasts is counteracted and a decrease in bone formation leads to bone loss. This second effect is associated with decreased serotonin signaling in the hypothalamus and increased SNS output. Accordingly, normalization of sympathetic output with a low dose of propranolol can prevent Flx-induced bone loss.

It should be noted that the two independent effects exerted by Flx on bone remodeling are not binary effects, and the 3- and 6-w time points are arbitrary points in what is a continuum of bone remodeling. Indeed, at the 3 w time point bone parameters already appear to be trending down, albeit not significantly, in the Flx- compared to veh-treated mice. Likewise, osteoclast surface is still trailing down after 6 w of treatment.

Brain serotonin, signaling through an Htr2c-CREB cascade, positively regulates bone mass accrual by inhibiting sympathetic output[13,14]. Thus, how can Flx mimic the effect of a decrease in brain serotonin signaling on bone remodeling while its canonical activity on 5HTT should increase this activity? In agreement with previous studies showing that high

concentrations of serotonin can desensitize Htr2c[42–44], our data show lower hypothalamic levels of phosphorylated CREB, its downstream mediator, upon 6 w of treatment with Flx compared to veh. In addition, mice treated with Flx for 3 and 6 w had progressively lower levels of hypothalamic Htr2c compared to veh-treated mice. Thus, with time, Flx decreases serotonin signaling in Htr2c neurons and thereby causes a similar, negative, effect on bone remodeling as the absence of brain serotonin[13,14]. This central-SNS–mediated detrimental activity on bone remodeling appears to be delayed compared to the direct, anti-resorptive, action of Flx. This difference in timing could stem from the fact that more time could be needed for this drug to cause an increase in inter-synaptic brain serotonin sufficient to desensitize the Htr2c receptor and decrease its expression than to reach osteoclasts peripherally and directly disturb their function.

An unexpected finding of our study is the fact that Flx can act directly on osteoclasts through a pathway different from its canonical mode of action. Although cells from the osteoclast lineage express the 5HTT transporter and the gene encoding Tph1, osteoclasts derived from mice lacking these genes respond to Flx similarly to wild-type cells[23,24,45]. Thus, at least in mice, Flx acts on these cells independently of the serotonin/5HTT system. Instead, this drug directly impairs Ca^{2+}-calmodulin signaling. This ability of Flx to interfere with intracellular Ca^{2+} homeostasis has been observed in other cell types[32,46,47]. Accordingly, Flx can impair extracellular Ca^{2+} influx by blocking various voltage-gated and ligand-gated ion channels[47–49]. More recently, Flx was also found to inhibit IP3- and ryanodine-receptor mediated Ca^{2+} release from intracellular stores in lymphocytes, an effect that could explain the poorly understood immunomodulatory activity of SSRIs[32,50–53]. Additional studies will be needed to determine which of these mechanisms occurs in osteoclasts. Further, through a simultaneous inhibition of osteoclast function and a decrease in Th17 lymphocyte activation[34,50,54], this mode of action could also explain the beneficial effect of SSRIs on multiple outcomes of osteoarthritis in mice and humans[55–57]. Again, additional studies are required to test this possibility.

More generally, considering that our study was performed using mouse models one cannot exclude that differences could exist between the mechanisms we describe in mice and those at play in humans taking SSRIs. Yet, the dual effect of Flx on bone remodeling we observe in our mouse models is consistent with data reported in the clinical literature. For instance, most clinical studies analyzed long-term SSRIs users and found a negative effect on bone health[5,6,9,11] consistent with the central effect of Flx on the sympathetic tone that we identified. In line with this notion, Flx increases the plasma concentration of E and NE in individuals[58] suggesting that, as in mice, decreasing sympathetic signaling in osteoblasts through the use of a β2-blocker could prevent bone loss in long-term users of SSRIs. Likewise, in agreement with the anti-resorptive activity of Flx, individuals evaluated shortly after taking SSRIs show higher calcaneal BMD T-score and lower serum concentration of the resorption biomarker CTx[15,16]. Lastly, we show that citalopram does not inhibit mouse osteoclast differentiation and others have reported that escitalopram, its S-enantiomer, did not affect bone resorption in nondepressed women treated for a short time with this drug[59]. These observations illustrate that SSRIs may not all have a similar impact on bone remodeling and that in animal studies as in clinical reports more attention should be given to potential intra-class differences.

Online Methods

Animals and *in vivo* treatments

We purchased males and females C57BL6/J and *Slc6a4*$^{-/-}$ mice from The Jackson Laboratories (Bar Harbor, Maryland). Generation of *Tph2*$^{-/-}$ mice was reported previously[13]. We generated *Tph1*$^{-/-}$ mice by crossing *Tph1*$^{fl/fl}$ mice[60] and EIIA-Cre. All mice were analyzed on the C57BL6/J background. We added fluoxetine hydrochloride USP (Flx, 20mg/kg/day, Voigt Global Distribution Inc., Lawrence, Kansas) and propranolol (Prop, 0.5mg/day, Sigma, St. Louis, Missouri) aseptically to the drinking water of virgin female or male mice. We treated mice for either 3 w or 6 w as indicated in each specific case, replacing bottles every other day. All mice were analyzed between the age of 17 and 20 weeks. Any mouse displaying immobility, huddled posture, inability to eat or drink, ruffled fur, self-mutilation, vocalization, wound dehiscence or signs of hypothermia was excluded from the study. In all experiments, animals were randomly assigned to the veh- or Flx-treated groups. For all assays, investigators were blinded to the type of treatment. The Columbia University Institutional Animal Care and Use Committee (IACUC) approved all procedures.

Measurement of biomarkers

We collected blood samples through cardiac puncture under Avertin anesthesia using Multivette 600 tubes from Sarstedt (Numbrecht, Germany) and centrifuged at 13,000 g for 10_ min at 4 °C. We measured the concentration of OCN with Ocn IRMA kit (Immutopics, San Clemente, California). We collected urine samples in the morning for at least three days within the week previous to sacrifice and measured the concentrations of Dpd with the Dpd EIA kit (Quidel, San Diego, California) and of E and NE with the Bi-CAT ELISA kit (Alpco, Salem, New Hampshire). We reported urine values to the concentration of Creatinine quantified with the Creatinine EIA kit (Quidel). We measured epinephrine content in brainstem by HPLC with a modified method described previously[61]. Briefly, dissected brain samples were homogenized in 0.4 M perchloric acid with an Ultra Cell Disruptor (Microson). The homogenate was centrifuged for 5 minutes at 14,000 g in cold room and a 50 µl of typically four-times diluted aliquot of the supernatant was injected over the HPLC system equipped with a Varian Microsorb 100-5 C18 reverse-phase column (DYNAMAX 150×4.6 mm). The mobile phase contained 0.75 mM sodium phosphate (pH 3.1), 1.4 mM 1-Octanesulfonic acid, 10 µM sodium EDTA and 8% acetonitrile and the flow rate was maintained at 0.8 ml/min. Values were calculated based on peak area and compared to standard solutions. The inter- and intra-assay coefficients of variation of the assay were each less than 5%. The sensitivity of the assay was less than 0.5 pmol/injection.

Cell culture, in vitro treatments and imaging

We obtained mouse primary osteoclast precursors (monocytes) by culturing bone marrow cells with M-CSF-containing L-929 (ATCC, Massanas, Virginia) cell supernatant (10%) for 5–6 days in DMEM 10% FBS. We then differentiated osteoclast precursors with 30 ng/mL of RANKL (R&D Systems Inc, Minneapolis, Minnesota) and 10 ng/mL of M-CSF (R&D) in αMEM 10% FBS for 6 days. We cultured RAW264.7 cells (ATCC) in DMEM 10% FBS and differentiated with 30 ng/mL of RANKL (R&D) in αMEM 10% FBS for 3 days before

Flx treatment. Medium was replaced every 48h. We isolated mouse primary osteoblasts from 3 day-old pups and cultured them with αMEM 10% FBS for 2 days as previously described[62]. Osteoblasts were differentiated in αMEM 10% FBS, 100 μg/ml L-ascorbic acid, 5 mM β-glycerophosphate for 6 days in presence of veh or Flx (3 μM). We cultured Neuro2A cells (ATCC) in DMEM 10% FBS and starved them in 0.5% FBS for 16–18 h before serotonin treatment. *Creb*$^{-/-}$ osteoclasts were generated by infecting *Creb*$^{fl/fl}$ cells with either empty vector or *Cre*-expressing adenovirus (1:800 MOI) (University of Iowa). We did not test the cultures of primary cells or cell lines for mycoplasma infection. Primary cell cultures were authenticated through gene expression analysis of specific markers.

We dissolved fluoxetine (Voigt Global Distribution Inc., Lawrence, Kansas), paroxetine, fluvoxamine and citalopram (Abcam, Cambridge, Massachusetts) at 10 mM in NaCl 0.9% and added them to the medium to the final concentration of 3 μM for 6 days (end point) or only during the last 24 h of culture. In 6 days treatment, medium was replaced every 48 h. We dissolved W-5 (Santa Cruz) at 10 mM in water and added it to the medium to the final concentration of 50 μM. We dissolved KG-501 (Sigma) at 10 mM in DMSO and added it to the medium to the final concentration of 10 μM. For detached live cells analysis, we treated cultures of mature osteoclasts for 24 h with fluoxetine or vehicle then we collected and centrifuged the media. We subjected the pellets to a TRAP assay or re-seeded them in new plates and cultured them in osteoclast differentiation medium until we stained the plates with TRAP (see below). For counting the number of nuclei/osteoclast, we fixed primary osteoclasts in 4% formaldehyde, stained actin with a 1:100 dilution of Alexa Fluor 548-conjugated phalloidin (Life Technologies, A12380) and nuclei with DAPI at 0.2 μg/ml (Life Technologies).

We imaged cultures under bright field (TRAP staining) or fluorescent light (actin) with a Leica DM400B (Wetzlar, Germany). We used ImageJ software to quantify the number of cells and nuclei for each osteoclast.

TRAP and Pit resorption assays

For TRAP staining, we fixed primary osteoclast cultures in 10% formalin, washed and incubated them with TRAP staining reagent (0.5 mg/ml Naphthol AS-MX Phosphate (Sigma), 0.4 mg/ml Fast Red Violet (Sigma) in acetate-tartrate buffer [25 mM Sodium acetate and 20 mM Sodium tartrate, pH5]) for 30 min at RT. For TRAP quantification in supernatant, we incubated 50 μl of culture medium for 1 h at 37 °C with 50 μl of 10 mM pNPP (Sigma) in TRAP assay buffer (200 mM Sodium chloride, 200 mM Sodium citrate and 80 mM of Sodium L-(+)-tartrate, pH5). We stopped the reaction by adding 50 μl of NaOH 3M and performed colorimetry at 405 nm vs a reference at 490 nm using a microplate reader (Bio-Rad 680, Hercules, California). We calculated TRAP activity as (Abs_{405} x vol (ml))/(ε x time (min)). ε (molar extinction coefficient) of pNPP is 17.8 $mM^{-1}cm^{-1}$. We processed and read technical duplicates of each sample. We performed pit resorption assays using Osteo Assay Stripwell Plates (Corning, New York, New York) following the manufacturer's protocol.

Gene expression, protein analyses and immunocytochemistry

We purified RNA from cells in culture and tissues using TRIzol (Invitrogen, Grand Island, New York) following the manufacturer's protocol. We flushed long bones of bone marrow prior to RNA purification. We performed real-time PCR (qPCR) using the Taq SYBR Green Power PCR Master Mix (Invitrogen) on a CFX Connect instrument (Bio-Rad, Hercules, California); *Gapdh* or *Hprt* (in case of brain samples) amplification was used as an internal reference for each sample. Verification of amplicon specificity was tested through a BLAST search and the size of amplicons was verified by gel electrophoresis. Dissociation curves analysis was performed for every experiment. Sequences of the primers used for each gene are available upon request.

We subjected protein extracts from cells or tissue to western blotting using the following antibodies: phospho-CREB in Figure 3f (1:1000, Cell Signaling, Danvers, Massachusetts, 9198), phospho-CREB in all other figures (1:1000, Merck Millipore, Billerica, Massachusetts, 06-519) CREB (1:1000, Cell Signaling, 9104), phospho-p38 MAPK (1:1000, Cell Signaling, 9211), p38 MAPK (Cell Signaling, 9212), IκBα (1:5000, Cell Signaling, 4814), GAPDH (1:5000, Cell Signaling, 5174), Htr2c (1:500, Santa Cruz sc-17797). We visualized immunocomplexes with a HPR-conjugated anti-rabbit or anti-mouse IgG antibody (1:2000) followed by incubation with ECL-Western blot reagent (GE Healthcare, Indianapolis, Indiana). Imaged blots were quantified using the ImageJ software (National Institutes of Health). Uncropped blots are presented in Supplementary Data Set 1. For all antibodies, validation is provided in manufacter's website.

For NF-κB p65 localization by immunocytochemistry, we grown RAW264.7 cells until differentiation and depleted them of RANKL for 1 h. Subsequently, we incubated for 30 min with indicated amounts of RANKL, and with vehicle or Flx as indicated. Then, we fixed them in 4% formaldehyde, incubated them in PBS 0.5% Triton-X-100 for permeabilization and then treated them with PBS 10% FBS to block nonspecific binding. We incubated them overnight at 4 °C with NFκB p65 antibody (1:400, Cell Signaling, 8242). We used Alexa Fluor 488-conjugated goat anti-rabbit (1:400, Life Technologies, A11006) as a secondary antibody. We stained actin with a dilution of Alexa Fluor 548-conjugated phalloidin (1:100) and nuclei with DAPI at 0.2 μg/ml. We used a Zeiss Axiovert 200 (Jena, Germany) to image and the ImageJ software to compose p65 nuclear translocation panels.

Calcium imaging with Fura-2

We cultured RAW264.7 cells on 35 mm glass bottom dishes (CellVis Ca, USA) and differentiated them with 30 ng/ml of RANKL (R&D) for 3 days. Before imaging, we loaded cells with 5 μM of calcium (Ca^{2+}) indicator Fura-2 for 45 min. At the moment of imaging, regular medium was replaced with phenol red free DMEM (CellGro Mediatech, Manassas, Virginia). We recorded intracellular Ca^{2+} levels as represented by ratio of Fura-2 (340/380 nm) absorbance in single cells of each culture using a Nikon Eclipse T*i* microscope equipped with a random access monochromator (Photon Technology International, PTI, Birmingham, New Jersey) for excitation and a Photometrics (Tucson, Arizona) QuantEM EM-CCD camera for image acquisition. We drawn regions of interest (ROI) around osteoclasts and mononuclear cells, and images were acquired using a 40X 1.3 NA oil

objective for a total of 8 min. We added 3 μM of fluoxetine (Flx) with a pipette at $t = 3$ min and 3 μM sarco/endoplasmics reticulum ATPase blocker, Thapsigargin (Thap) (Sigma, St. Louis, Missouri) at $t = 6$ min. We used increased cytosolic Ca^{2+} concentration by Thap as a positive control of cell viability. Only cells exhibiting a positive response to Thap were subsequently analyzed for Flx effect. We analyzed Fura-2 ratio in the acquired images using Easy Ratio Pro software (PTI). We then represented Flx-induced decreased of intracellular Ca^{2+} levels as the area under the curve (AUC), calculated relatively to the lowest value of each curve.

Bone histomorphometry and micro-computed tomography

We dissolved calcein (Sigma, St. Louis, Missouri) in 0.15 M NaCl, 2% $NaHCO_3$ and injected it intraperitoneally at 0.025 mg/g body weight on days 1 and 4, then we sacrificed mice on day 6. For bone histomorphometric analysis, we fixed L3–L4 vertebrae and tibiae for 24_hours in 10% formalin, dehydrated them in a graded series of ethanol, and embedded them in methyl methacrylate resin. We performed a Von Kossa/van Gieson staining on 7 μm sections for the quantification of bone volume over tissue volume (BV/TV) using the ImageJ software (Bethesda, Maryland). We took the pictures using a Leica DM400B (Wetzlar, Germany) or Olympus BX53 (Tokyo, Japan). We analyzed bone formation rate (BFR) on 5μm sections using calcein labeling. For analysis of the parameters of osteoblasts and osteoclasts, we stained 5μm sections with toluidine blue and tartrate-resistant acid phosphatase (TRAP), respectively. We performed histomorphometry analysis using the Osteomeasure Analysis System from Osteometrics (Atlanta, Georgia). We performed micro-computed tomography to analyze trabecular morphological parameters of the proximal tibia (VivaCT 40, Scanco Medical AG, Bassersdorf, Switzerland). Briefly, energy settings were 55 kV, and 109 μA, and reconstructed images had a 10.5 μm isotropic voxel size. The region of interest was defined starting at the growth plate and extending approximately 1 mm distally. Prior to analysis, a Gaussian filter was applied (sigma =.8, support =1) to reduce noise. A global threshold of 30% of the maximum gray scale value was used to classify bone. Standard Scanco evaluation software utilizing a distance transformation method was used in the calculation of output variables.

Marble burying test

We performed tests 1 day before sacrifice. We placed twenty glass marbles, evenly spaced in five rows, on approx. 5-cm layer of sawdust bedding lightly pressed down to make a flat even surface, in a plastic cage. Then, we placed the mouse in the cage and left it for 30min after which the number of marbles buried with sawdust was counted[63,64].

Statistical analysis

We expressed all values as mean + SEM. We determined group sizes by performing a power calculation to lead to an 80% chance of detecting a significant difference ($p \leq 0.05$). All values use biological replicates and are indicated by group size (n) in figure legends or within bar graphs. For *in vivo* data, each "*n*" corresponds to a single mouse. For *in vitro* data, each "*n*" corresponds an independent experiment. If technical replicates were performed their mean was considered as one "*n*". Statistical analyses were performed using one-way ANOVA followed by Turkey's or Dunnet's multiple comparison tests to compare

means of three or more groups; and unpaired two-tailed Student's t-test to compare means of two groups. Variances were similar between groups. In all figures $*P \leq 0.05$, $**P \leq 0.01$, $***P \leq 0.001$, $****P \leq 0.0001$. Analysis were performed using GraphPad Prism (GraphPad Software) for ANOVA and Excel (Microsoft) for Student's t -test.

Supplementary Material

Refer to Web version on PubMed Central for supplementary material.

Acknowledgments

We thank Na Luo for help with histomorphometry, Timothy Hanna for handling the mouse colony and G. Karsenty and S. Kousteni for critical reading of the manuscript. The National Institute of Health grant AG032959 (PD) supported this work.

References

1. Wong DT, Bymaster FP, Engleman EA. Prozac (fluoxetine, lilly 110140), the first selective serotonin uptake inhibitor and an antidepressant drug: Twenty years since its first publication. Life Sciences. 1995; 57:411–441. [PubMed: 7623609]
2. Fox M, et al. A pharmacological analysis of mice with a targeted disruption of the serotonin transporter. Psychopharmacology. 2007; 195:147–166. [PubMed: 17712549]
3. Mojtabai R, Olfson M. Proportion of antidepressants prescribed without a psychiatric diagnosis is growing. Health affairs (Project Hope). 2011; 30:1434–1442. [PubMed: 21821561]
4. Orleans RJ, et al. FDA Approval of Paroxetine for Menopausal Hot Flushes. New England Journal of Medicine. 2014; 370:1777–1779. [PubMed: 24806158]
5. Rizzoli R, et al. Antidepressant medications and osteoporosis. Bone. 2012; 51:606–613. [PubMed: 22659406]
6. Haney EM, Warden SJ, Bliziotes MM. Effects of selective serotonin reuptake inhibitors on bone health in adults: Time for recommendations about screening, prevention and management? Bone. 2010; 46:13–17. [PubMed: 19664737]
7. Wu Q, Magnus JH, Liu J, Bencaz AF, Hentz JG. Depression and low bone mineral density: a meta-analysis of epidemiologic studies. Osteoporosis International. 2009; 20:1309–1320. [PubMed: 19343469]
8. Warden SJ, Nelson IR, Fuchs RK, Bliziotes MM, Turner CH. Serotonin (5-hydroxytryptamine) transporter inhibition causes bone loss in adult mice independently of estrogen deficiency. Menopause. 2008; 15:1176–1183. [PubMed: 18725867]
9. Warden SJ, Robling AG, Sanders MS, Bliziotes MM, Turner CH. Inhibition of the serotonin (5-hydroxytryptamine) transporter reduces bone accrual during growth. Endocrinology. 2005; 146:685–693. [PubMed: 15539550]
10. Bonnet N, et al. Various effects of antidepressant drugs on bone microarchitectecture, mechanical properties and bone remodeling. Toxicol Appl Pharmacol. 2007; 221:111–118. [PubMed: 17383703]
11. Bliziotes M, Gunness M, Eshleman A, Wiren K. The role of dopamine and serotonin in regulating bone mass and strength: studies on dopamine and serotonin transporter null mice. Journal of musculoskeletal & neuronal interactions. 2002; 2:291–295. [PubMed: 15758457]
12. Gebara MA, et al. Depression, Antidepressants, and Bone Health in Older Adults: A Systematic Review. Journal of the American Geriatrics Society. 2014; 62:1434–1441. [PubMed: 25039259]
13. Yadav VK, et al. A serotonin-dependent mechanism explains the leptin regulation of bone mass, appetite, and energy expenditure. Cell. 2009; 138:976–989. [PubMed: 19737523]
14. Oury F, et al. CREB mediates brain serotonin regulation of bone mass through its expression in ventromedial hypothalamic neurons. Genes & development. 2010; 24:2330–2342. [PubMed: 20952540]

15. Seifert CF, Wiltrout TR. Calcaneal Bone Mineral Density in Young Adults Prescribed Selective Serotonin Reuptake Inhibitors. Clinical Therapeutics. 2013; 35:1412–1417. [PubMed: 23958172]
16. Aydin H, Mutlu N, Akbas NBG. Treatment of a major depression episode suppresses markers of bone turnover in premenopausal women. Journal of Psychiatric Research. 2011; 45:1316–1320. [PubMed: 21531430]
17. Misra M, et al. Use of SSRIs may Impact Bone Density in Adolescent and Young Women with Anorexia Nervosa. CNS spectrums. 2010; 15:579–586. [PubMed: 24790401]
18. Bolo NR, et al. Brain pharmacokinetics and tissue distribution in vivo of fluvoxamine and fluoxetine by fluorine magnetic resonance spectroscopy. Neuropsychopharmacology. 2000; 23:428–438. [PubMed: 10989270]
19. Boyce BF. Advances in the Regulation of Osteoclasts and Osteoclast Functions. Journal of Dental Research. 2013; 92:860–867. [PubMed: 23906603]
20. Teitelbaum SL, Ross FP. Genetic regulation of osteoclast development and function. Nat Rev Genet. 2003; 4:638–649. [PubMed: 12897775]
21. Zou W, et al. Talin1 and Rap1 Are Critical for Osteoclast Function. Molecular and cellular biology. 2013; 33:830–844. [PubMed: 23230271]
22. Fukunaga T, Zou W, Warren JT, Teitelbaum SL. Vinculin Regulates Osteoclast Function. Journal of Biological Chemistry. 2014; 289:13554–13564. [PubMed: 24675074]
23. Battaglino R, et al. Serotonin Regulates Osteoclast Differentiation Through Its Transporter. Journal of Bone and Mineral Research. 2004; 19:1420–1431. [PubMed: 15312242]
24. Hodge JM, et al. Selective Serotonin Reuptake Inhibitors Inhibit Human Osteoclast and Osteoblast Formation and Function. Biological Psychiatry. 2013; 74:32–39. [PubMed: 23260229]
25. Fuller RW, Wong DT. Serotonin uptake and serotonin uptake inhibition. Annals of the New York Academy of Sciences. 1990; 600:68–78. discussion 79–80. [PubMed: 2252338]
26. Takayanagi H. Osteoimmunology: shared mechanisms and crosstalk between the immune and bone systems. Nat Rev Immunol. 2007; 7:292–304. [PubMed: 17380158]
27. Chen W, et al. C/EBPα regulates osteoclast lineage commitment. Proceedings of the National Academy of Sciences. 2013; 110:7294–7299.
28. Sato K, et al. Regulation of osteoclast differentiation and function by the CaMK-CREB pathway. Nature medicine. 2006; 12:1410–1416.
29. Kuroda Y, Hisatsune C, Nakamura T, Matsuo K, Mikoshiba K. Osteoblasts induce Ca2+ oscillation-independent NFATc1 activation during osteoclastogenesis. Proceedings of the National Academy of Sciences. 2008; 105:8643–8648.
30. Hidaka H, Asano M, Tanaka T. Activity-structure relationship of calmodulin antagonists, Naphthalenesulfonamide derivatives. Mol Pharmacol. 1981; 20:571–578. [PubMed: 7329399]
31. Best JL, et al. Identification of small-molecule antagonists that inhibit an activator: coactivator interaction. Proc Natl Acad Sci U S A. 2004; 101:17622–17627. [PubMed: 15585582]
32. Gobin V, et al. Fluoxetine suppresses calcium signaling in human T lymphocytes through depletion of intracellular calcium stores. Cell Calcium. 2015; 58:254–263. [PubMed: 26115837]
33. Okamoto K, Takayanagi H. Regulation of bone by the adaptive immune system in arthritis. Arthritis Res Ther. 2011; 13:219. [PubMed: 21635718]
34. Takayanagi H. New developments in osteoimmunology. Nat Rev Rheumatol. 2012; 8:684–689. [PubMed: 23070645]
35. Karsenty G, Kronenberg HM, Settembre C. Genetic control of bone formation. Annu Rev Cell Dev Biol. 2009; 25:629–648. [PubMed: 19575648]
36. Karsenty G, Ferron M. The contribution of bone to whole-organism physiology. Nature. 2012; 481:314–320. [PubMed: 22258610]
37. Wada T, Nakashima T, Hiroshi N, Penninger JM. RANKL–RANK signaling in osteoclastogenesis and bone disease. Trends in molecular medicine. 2006; 12:17–25. [PubMed: 16356770]
38. Ruocco MG, et al. IκB kinase (IKK)β, but not IKKα, is a critical mediator of osteoclast survival and is required for inflammation-induced bone loss. The Journal of experimental medicine. 2005; 201:1677–1687. [PubMed: 15897281]

39. Takeda S, et al. Leptin regulates bone formation via the sympathetic nervous system. Cell. 2002; 111:305–317. [PubMed: 12419242]
40. Elefteriou F, et al. Leptin regulation of bone resorption by the sympathetic nervous system and CART. Nature. 2005; 434:514–520. [PubMed: 15724149]
41. Gainetdinov RR, Premont RT, Bohn LM, Lefkowitz RJ, Caron MG. Desensitization of G protein-coupled receptors and neuronal functions. Annu Rev Neurosci. 2004; 27:107–144. [PubMed: 15217328]
42. Bristow LJ, O'Connor D, Watts R, Duxon MS, Hutson PH. Evidence for accelerated desensitisation of 5-HT2C receptors following combined treatment with fluoxetine and the 5-HT1A receptor antagonist, WAY 100,635, in the rat. Neuropharmacology. 2000; 39:1222–1236. [PubMed: 10760364]
43. Yamauchi M, Tatebayashi T, Nagase K, Kojima M, Imanishi T. Chronic treatment with fluvoxamine desensitizes 5-HT2C receptor-mediated hypolocomotion in rats. Pharmacology Biochemistry and Behavior. 2004; 78:683–689.
44. Kennett GA, et al. Effect of chronic administration of selective 5-hydroxytryptamine and noradrenaline uptake inhibitors on a putative index of 5-HT2C/2B receptor function. Neuropharmacology. 1994; 33:1581–1588. [PubMed: 7760981]
45. Chabbi-Achengli Y, et al. Decreased osteoclastogenesis in serotonin-deficient mice. Proc Natl Acad Sci U S A. 2012; 109:2567–2572. [PubMed: 22308416]
46. Kim HJ, et al. Fluoxetine suppresses synaptically induced [Ca2+]i spikes and excitotoxicity in cultured rat hippocampal neurons. Brain Research. 2013; 1490:23–34. [PubMed: 23131584]
47. Deak F, et al. Inhibition of voltage-gated calcium channels by fluoxetine in rat hippocampal pyramidal cells. Neuropharmacology. 2000; 39:1029–1036. [PubMed: 10727713]
48. Hahn SJ, et al. Inhibition by fluoxetine of voltage-activated ion channels in rat PC12 cells. Eur J Pharmacol. 1999; 367:113–118. [PubMed: 10082273]
49. Kecskemeti V, et al. Norfluoxetine and fluoxetine have similar anticonvulsant and Ca2+ channel blocking potencies. Brain research bulletin. 2005; 67:126–132. [PubMed: 16140171]
50. Shenoy AR, et al. Citalopram suppresses thymocyte cytokine production. Journal of Neuroimmunology. 2013; 262:46–52. [PubMed: 23886473]
51. Kubera M, Kenis G, Bosmans E, Scharpe S, Maes M. Effects of serotonin and serotonergic agonists and antagonists on the production of interferon-gamma and interleukin-10. Neuropsychopharmacology. 2000; 23:89–98. [PubMed: 10869889]
52. Branco-de-Almeida LS, et al. Fluoxetine inhibits inflammatory response and bone loss in a rat model of ligature-induced periodontitis. Journal of Periodontology. 2012; 83:664–671. [PubMed: 21966942]
53. Pellegrino TC, Bayer BM. Modulation of Immune Cell Function Following Fluoxetine Administration in Rats. Pharmacology Biochemistry and Behavior. 1998; 59:151–157.
54. Schett G, Teitelbaum SL. Osteoclasts and Arthritis. Journal of Bone and Mineral Research. 2009; 24:1142–1146.
55. Baharav E, et al. Immunomodulatory Effect of Sertraline in a Rat Model of Rheumatoid Arthritis. Neuroimmunomodulation. 2012; 19:309–318. [PubMed: 22797111]
56. Hochberg MC, Wohlreich M, Gaynor P, Hanna S, Risser R. Clinically Relevant Outcomes Based on Analysis of Pooled Data from 2 Trials of Duloxetine in Patients with Knee Osteoarthritis. The Journal of Rheumatology. 2012; 39:352–358. [PubMed: 22133624]
57. Sacre S, Medghalchi M, Gregory B, Brennan F, Williams R. Fluoxetine and citalopram exhibit potent antiinflammatory activity in human and murine models of rheumatoid arthritis and inhibit toll-like receptors. Arthritis & Rheumatism. 2010; 62:683–693. [PubMed: 20131240]
58. Blardi P, et al. Plasma catecholamine levels after fluoxetine treatment in depressive patients. Neuropsychobiology. 2005; 51:72–76. [PubMed: 15741747]
59. Diem SJ, et al. Effects of escitalopram on markers of bone turnover: a randomized clinical trial. The Journal of clinical endocrinology and metabolism. 2014; 99:E1732–1737. [PubMed: 25014001]
60. Yadav VK, et al. Lrp5 controls bone formation by inhibiting serotonin synthesis in the duodenum. Cell. 2008; 135:825–837. [PubMed: 19041748]

61. Underwood MD, Arango V, Bakalian MJ, Ruggiero DA, Mann JJ. Dorsal raphe nucleus serotonergic neurons innervate the rostral ventrolateral medulla in rat. Brain Res. 1999; 824:45–55. [PubMed: 10095041]

62. Ducy P, Karsenty G. Two distinct osteoblast-specific cis-acting elements control expression of a mouse osteocalcin gene. Molecular and cellular biology. 1995; 15:1858–1869. [PubMed: 7891679]

63. Angoa-Perez M, Kane MJ, Briggs DI, Francescutti DM, Kuhn DM. Marble burying and nestlet shredding as tests of repetitive, compulsive-like behaviors in mice. J Vis Exp. 2013:50978. [PubMed: 24429507]

64. Nicolas LB, Kolb Y, Prinssen EPM. A combined marble burying–locomotor activity test in mice: A practical screening test with sensitivity to different classes of anxiolytics and antidepressants. European Journal of Pharmacology. 2006; 547:106–115. [PubMed: 16934246]

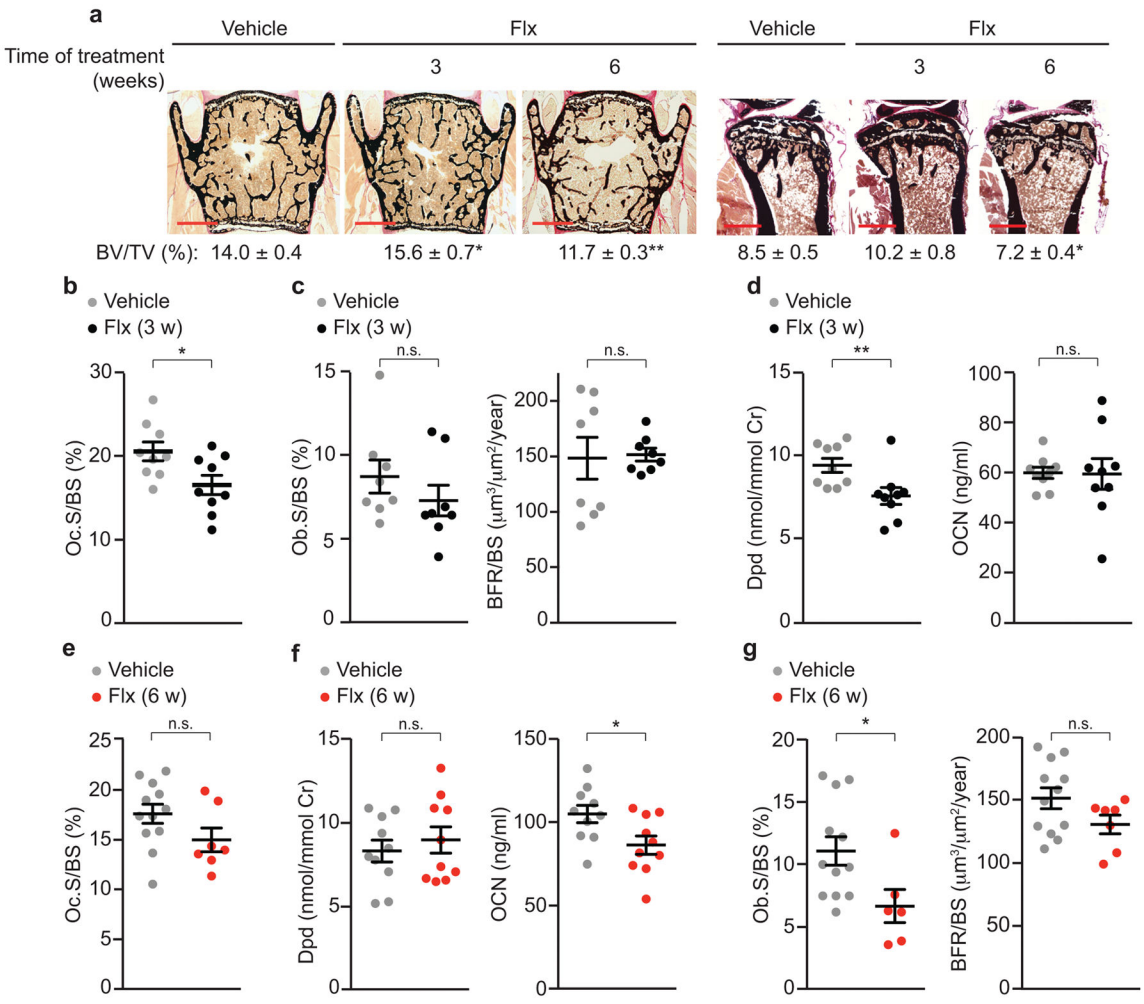

Figure 1. Biphasic effect of Flx on bone mass

(**a**) Representative images ($n = 4$ images/mouse) of vertebrae and quantification of BV/TV of WT female mice treated with Flx or veh for 3 or 6 weeks (veh $n = 10$, 3 w Flx $n = 10$, 6 w Flx $n = 16$) and tibiae (veh $n = 8$, 3 w Flx $n = 8$, 6 w Flx $n = 9$). Scale bars, 400 µm. (**b**–**d**) WT female mice treated with Flx or veh for 3 w. Vertebrae bone histomorphometry as measured by Oc.S/BS (**b**), Ob.S/BS, and BFR/BS (**c**). Urine concentration of Dpd crosslinks and plasma concentration of OCN (**d**). Cr, creatinine. Oc.S, osteoclast surface; BS, bone surface; Ob.S, osteoblast surface; BFR, bone formation rate. (**e**–**g**) WT female mice treated with Flx or veh for 6 w. Quantification of osteoclast surface in vertebrae (**e**), urine concentration of Dpd and plasma concentration of OCN (**f**) and bone histomorphometry of vertebrae as in **c** (**g**). Values are mean ± SEM compared to veh $*P \leq 0.05$, $**P \leq 0.01$ using a one-way ANOVA followed by Dunnet's test to veh (**a**, right) or Student's test (all other panels).

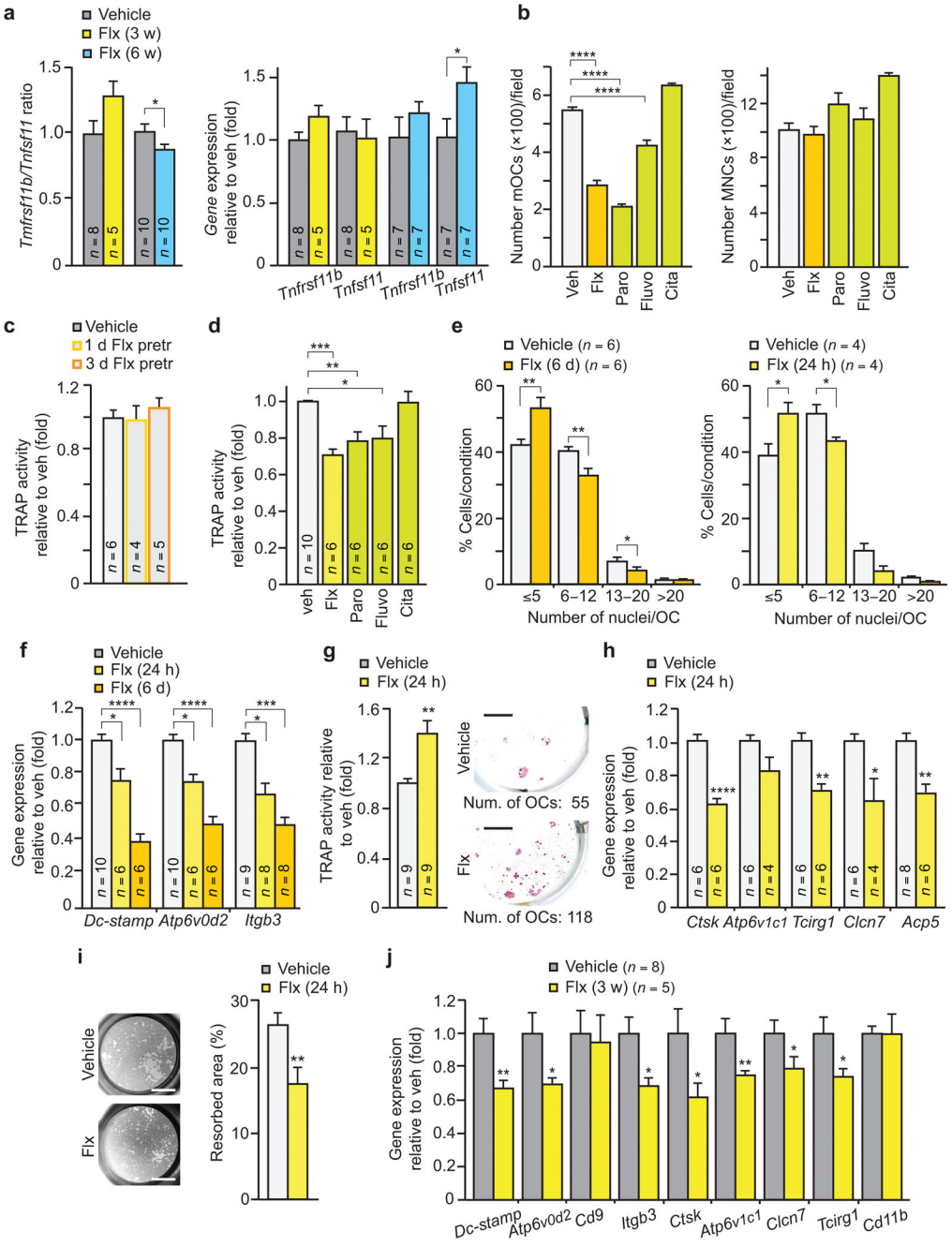

Figure 2. Flx directly impairs osteoclast differentiation and function

(**a**) *Tnfrsf11b*/*Tnfsf11* ratio and gene expression in long bones of WT female mice. (**b**) Effects of indicated SSRIs on the development of mature osteoclasts (mOCs) ($n = 4$) (left) and mononuclear cells (MNCs) ($n = 6$) (right) in primary osteoclast cultures (OCs) treated for 6 days. (**c**) Quantification of TRAP activity in primary OCs treated for 1 or 3 days (1 d, 3 d Flx pretr) with veh or Flx then subsequently grown in untreated medium until assayed at day 6. (**d**) Quantification of TRAP activity in primary OCs treated for 24 h. (**e**–**i**) Primary OCs assayed for the number of nuclei per cell (**e**), gene expression of osteoclast fusion

markers and *Itgb3* (**f**), TRAP activity (left) and TRAP staining after subculture (right; scale bars, 4 mm) (**g**), gene expression of resorbing activity markers (*Ctsk, Cathepsin K. Clcn7, Chloride channel 7. Acp5* encodes TRAP) (**h**), and pit resorption activity, with representative images ($n = 8$ images/condition) (left) and quantified percentage of resorbed area ($n = 8$) (right) (**i**). Scale bars, 2 mm. (**j**) Gene expression analysis of long bones of females treated for 3 w. Values are mean ± SEM compared to veh $^{*}P \leq 0.05$, $^{**}P \leq 0.01$, $^{***}P \leq 0.001$, $^{****}P \leq 0.0001$ using one-way ANOVA followed by Dunnet's test (**b**,**d**,**f**) or Student's test (all other panels).

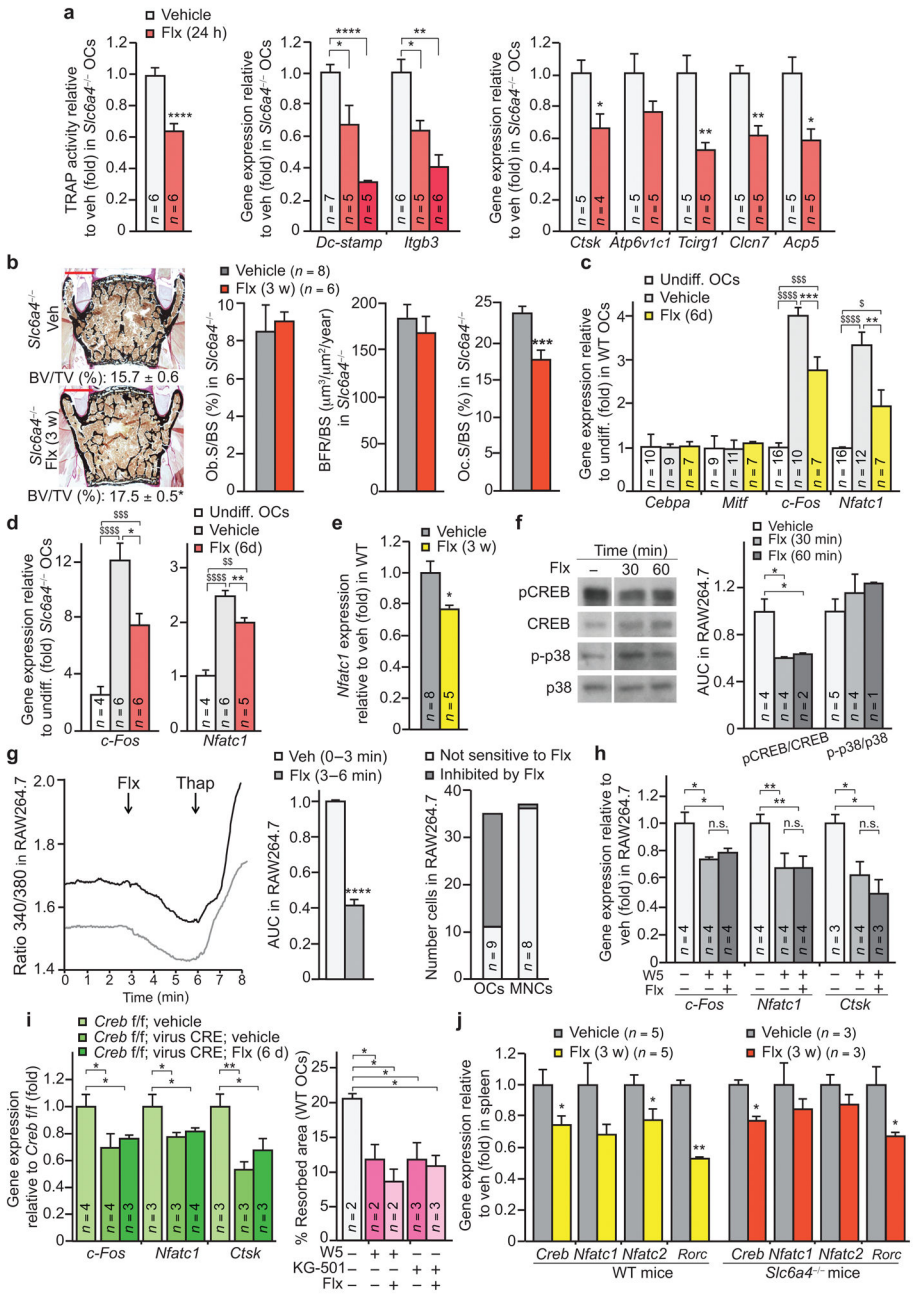

Figure 3. Flx affects osteoclastogenesis in a 5HTT-independent manner

(**a**) Quantification of TRAP activity (left) and gene expression in primary osteoclast cultures (OCs) derived from 5HTT-deficient (*Slc6a4*$^{-/-}$) mice. *Ctsk, Cathepsin K. Clcn7, Chloride channel 7. Acp5* encodes TRAP. (**b**) Representative images (n = 4 images/mouse) of vertebrae (left) from *Slc6a4*$^{-/-}$ females treated for 3 w (veh n = 8, Flx n = 6). Quantification of BV/TV is indicated below each image. Scale bars, 200 μm. Bone histomorphometry of these mice is also indicated (middle and right). (**c**,**d**) Gene expression in WT OCs (**c**) and *Slc6a4*$^{-/-}$ OCs (**d**). *Mitf* encodes microphthalmia-associated transcription factor; Undiff., undifferentiated OCs. (**e**) Expression of *Nfatc1* in long bones of WT females treated for 3 w.

(**f**) Western blot (left) and quantification of band intensities reported to veh (right) of indicated proteins in RAW264.7 osteoclasts treated with Flx or veh (n = 1 technical replicate of the number of biological replicates indicated in the bar graph (left)). (**g**) Representative curves (n = 13) of Fura-2 ratio (340/380) in individual RAW264.7 osteoclasts recorded in veh medium and after addition of Flx (left), Fura-2 ratio levels after Flx addition relative to veh (AUC, area under the curve (n = 13) (middle), and proportion of OCs and MNCs responding to Flx (right). Thap, Thapsigargin. (**h**) Gene expression in RAW264.7 osteoclasts treated for 24 h. (**i**) Gene expression in *Creb* fl/fl:virus-CRE OCs treated for 6 days (6 d) (left), and the percentage of resorbed area in a pit resorption assay of WT OCs treated for 24 h with W5, KG-501 and Flx (right). (**j**) Gene expression in spleen of WT or *Slc6a4*$^{-/-}$ females treated for 3 weeks. *Rorc* encodes RORγt. Values are mean ± SEM compared to veh (*) or undiff. OCs ($) */$$P \leq 0.05$, **$P \leq 0.01$, ***/$$$P \leq 0.001$, ****/$$$$P \leq 0.0001$. One-way ANOVA followed by Dunnet's test (**a**,**i**), one-way ANOVA followed by Turkey's (**c**,**d**,**h**) or Student's test (all other panels).

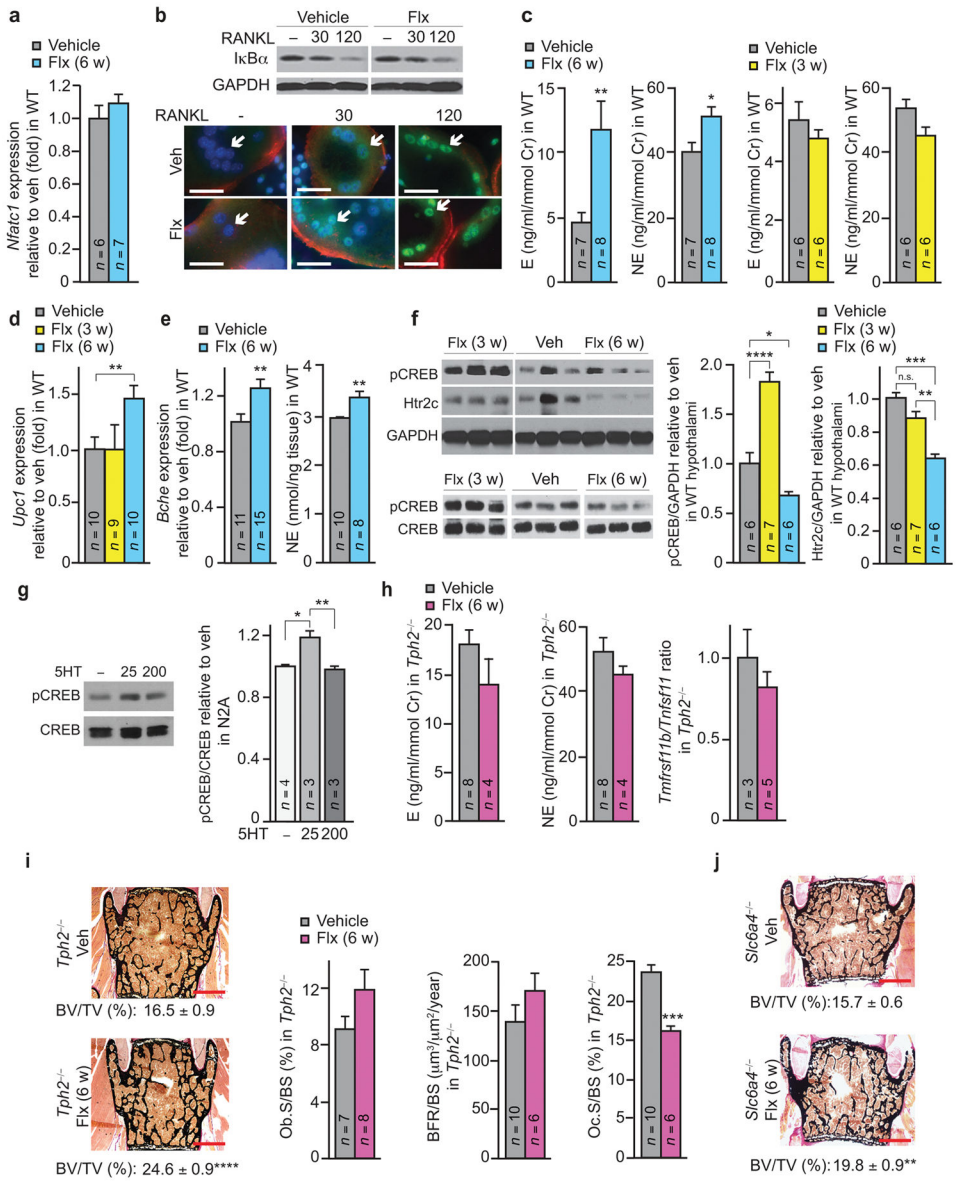

Figure 4. Flx-induced bone loss is brain serotonin-dependent and mediated by the sympathetic tone

(**a**) Expression of *Nfatc1* in long bones of WT females treated for 6 w. (**b**) Analysis of NF-κB signaling in RAW264.7 osteoclasts treated with RANKL (ng/ml), and with veh or Flx for 30 min. Top: Representative image of a western blot ($n = 2$ western blot per conditions). Bottom: NFκB-p65 (green) subcellular localization by immunocytochemistry. AF-548 phalloidine (actin, red), DAPI (nuclei, blue) ($n = 10$ images per group). Scale bar, 50 μm. Arrows indicate osteoclast nuclei. (**c**–**f**) WT female mice treated with Flx or veh for 3 or 6 weeks. Urine E and NE concentration (**c**), *Ucp1* expression in brown adipose tissue (**d**), *Bche* expression in hypothalamus (left) and NE content in brainstem (right) (**e**), western blot analysis of hypothalamus extracts ($n = 1$ technical replicate of the number of mice indicated in the bar graphs on the right, each lane shown corresponds to a single mouse) (left) and quantification of band intensities normalized with GAPDH and reported to veh (right) (**f**).

(**g**) Western blot analysis of Neuro2A (N2A) neuroblastoma cultures treated for 20 min with serotonin (μM) (veh $n = 4$, 25 and 200 5HT $n = 3$ western blots per condition). (**h**,**i**) Urine E (left) and NE (middle) concentrations and the *Tnfrsf11b*/*Tnfsf11* ratio in long bones (right) (**h**), and vertebrae analysis, with representative images ($n = 4$ images/mouse; scale bars, 400 μm) and quantification of BV/TV (left) and bone histomorphometric analyses (right) (i) in *Tph2*$^{-/-}$ females treated for 6 w. (veh $n = 10$, Flx $n = 8$). (**j**) Representative images of vertebrae ($n = 4$ images/mouse; scale bars, 400 μm) and quantification of BV/TV in *Slc6a4*$^{-/-}$ females treated for 6 w (veh $n = 8$, Flx $n = 4$). Values are mean ± SEM compared to veh $^{*}P \leq 0.05$, $^{**}P \leq 0.01$, $^{****}P \leq 0.0001$. One-way ANOVA followed by Dunnet's test (f, middle), followed by Turkey's test (f, right; g), or Student's test (all other panels).

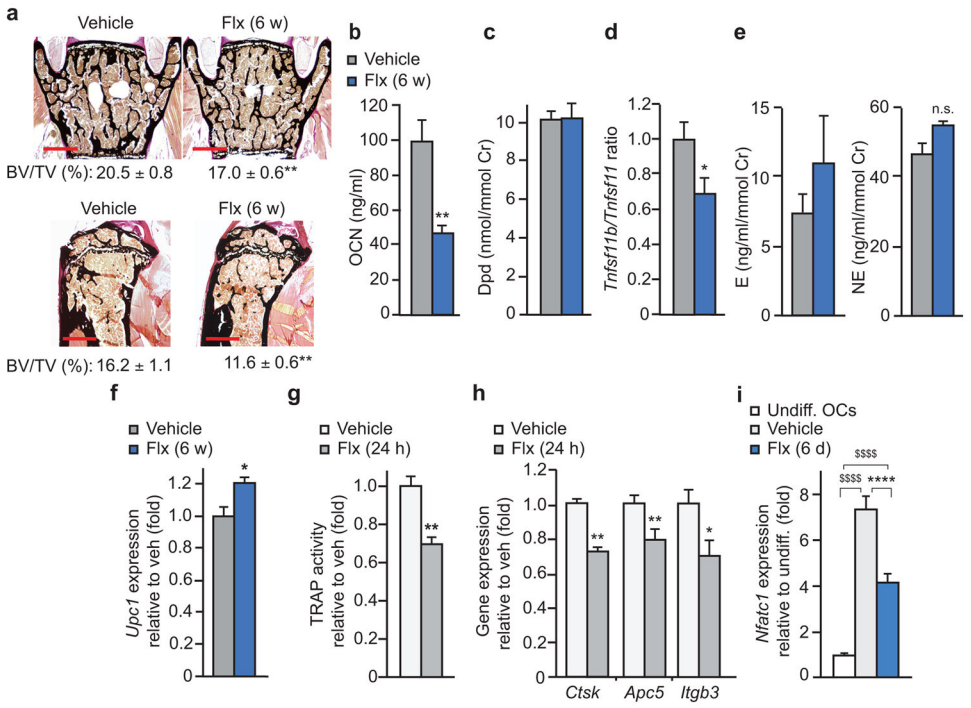

Figure 5. Flx-induced bone loss mediated by the sympathetic tone occurs also in males

All the male mice were WT and treated for 6 w. (**a**) Representative images ($n = 4$ images/mouse; scale bars, 400 μm) of vertebrae (top panels, $n = 9$ mice) and tibiae (bottom panels, $n = 10$ mice) and quantification of BV/TV. (**b**) Plasma concentration of OCN (veh $n = 9$, 6 w Flx $n = 7$). (**c**) Urine Dpd crosslinks concentration ($n = 6$). Cr, creatinine. (**d**) *Tnfrsf11b*/*Tnfsf11* expression ratio in long bones ($n = 8$). (**e**) Urine E and NE concentration ($n = 4$). (**f**) *Ucp1* expression in brown adipose tissue ($n = 7$). (**g-i**) Quantification of TRAP activity ($n = 4$) (**g**), gene expression of osteoclast resorbing activity and adhesion markers (veh $n = 6$, Flx $n = 4$) (**h**), and expression of *Nfatc1* ($n = 6$) (**i**) in primary osteoclast (OCs) cultures derived from WT male mice. Undiff., undifferentiated OCs. Values are mean ± SEM compared to veh (*) or to undiff. ($) */$ $P \leq 0.05$, **/$$ $P \leq 0.01$, **** $P \leq 0.0001$ using one-way ANOVA follow by Turkey's test (**i**) or Student's test (all other panels).

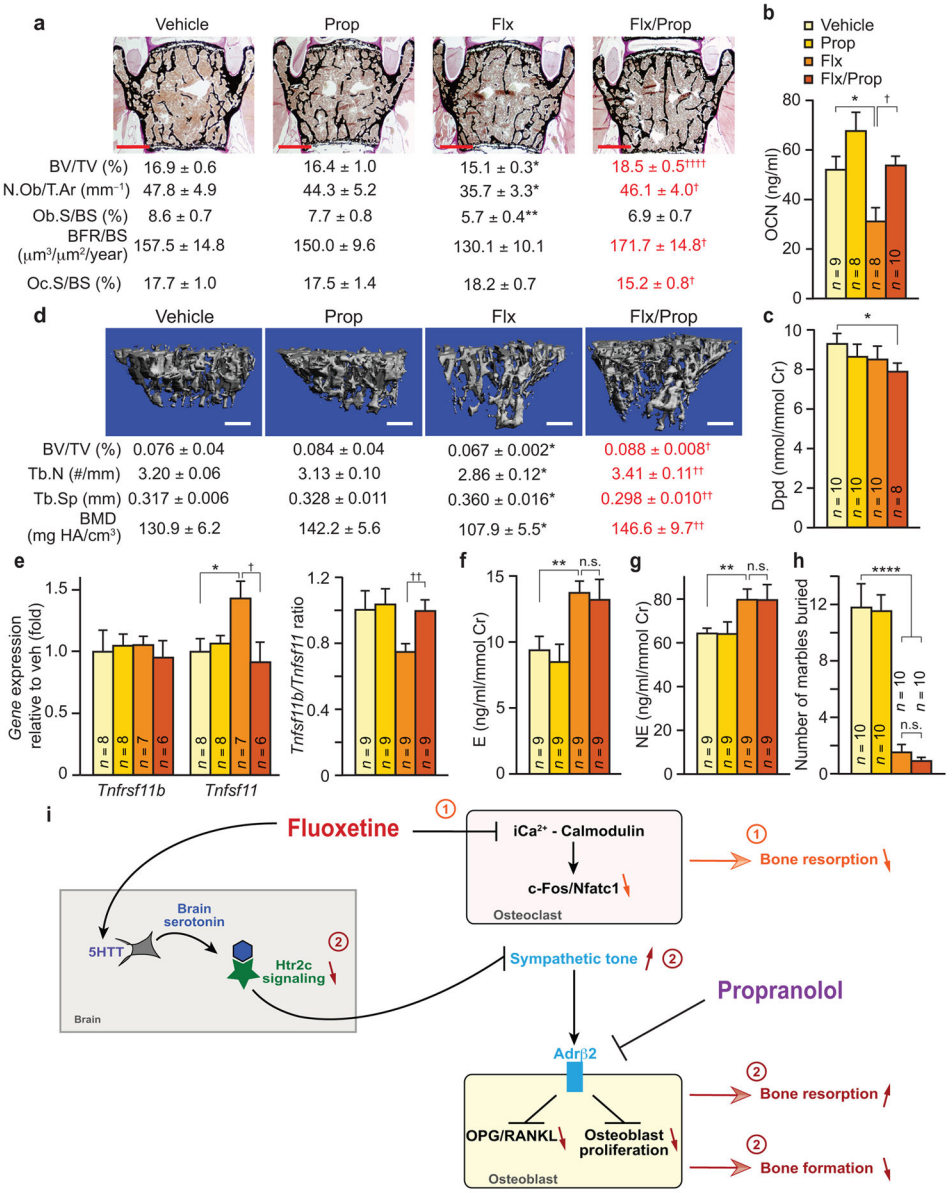

Figure 6. Co-treatment with propranolol rescues the Flx-induced bone loss

WT females treated for 6 w with vehicle (veh), Flx, Prop or a combination of both drugs (Flx/Prop). (**a**) Vertebrae analysis, with representative images (n = 4 images/mouse; scale bars, 400 µm) and quantification of BV/TV (veh n = 8, Flx, Prop and Flx/Prop n = 9) (top) and bone histomorphometric analyses (n = 6 or 8) (bottom). Scale bars, 400 µm. (**b**) Plasma concentration of OCN. (**c**) Urine concentration of Dpd crosslinks. Cr, creatinine. (**d**) Analysis of femurs by microcomputed tomography. Tb.N, trabecular number. Tb.Sp, trabecular spacing. BMD, bone mineral density (veh and Prop n = 10, Flx and Flx/Prop n = 9). Scale bars, 400 µm. (**e**) *Tnfrsf11b* and *Tnfsf11* expression and *Tnfrsf11b*/*Tnfsf11* ratio in long bones. (**f**) Urine E and (**g**) NE concentration. (**h**) Marble burying test. Values are mean ± SEM. In all panels, (†) represents Flx vs. Flx/Prop groups, (*) represents veh vs. Flx groups. †/*$P \leq 0.05$, ††/**$P \leq 0.01$, ††††/****$P \leq 0.0001$ using Student's tests. (**i**) Schematic

diagram of Flx mechanism of action on bone remodeling. Flx directly acts on osteoclasts to limit the Ca2+/calmodulin-dependent activation of the c-Fos-Nfatc1 cascade causing a decrease in bone resorption ①, independently of 5HTT. Also, through its inhibition of serotonin reuptake by 5HTT, Flx increases brain serotonin post-synaptic signaling causing the desensitization of Htr2c ②. As a result, sympathetic output increases, bone resorption increases and bone formation decreases. Upon a short exposure to fluoxetine the direct effect ① is predominant causing an increase in bone mass by decreasing bone resorption. Following a longer treatment, direct ① and central ② effects counteract each other in term of bone resorption while bone formation decreases, causing bone loss. The deleterious central effect of fluoxetine ② on bone remodeling can be prevented by a co-treatment with propranolol, which blocks the increase in Adrb2 signaling in osteoblasts caused by the higher sympathetic tone.